Bias effects on the electro-optic response of Ge-on-Si waveguide photodetectors

Bias effects on the electro-optic response of Ge-on-Si waveguide photodetectors

Matteo G. C. Alasio*, Michele Goano*†, Alberto Tibaldi*†, Francesco Bertazzi*†, Soha Namnabat‡, Donald Adams‡, Prakash Gothoskar‡, Fabrizio Forghieri‡, Giovanni Ghione*, Marco Vallone*
* Dipartimento di Elettronica e Telecomunicazioni, Politecnico di Torino, corso Duca degli Abruzzi 24, 10129 Torino, Italy
† IEIIT-CNR, corso Duca degli Abruzzi 24, 10129 Torino, Italy
‡ Cisco Systems, 7540 Windsor Drive, Suite 412, Allentown, PA 18195, USA
E-mail: michele.goano@polito.it

Abstract

We compare measurements and three-dimensional multiphysics simulations of the electro-optic frequency response of two vertical-pin-junction Ge-on-Si waveguide photodetectors at different bias voltages. The very good agreement observed even with no applied bias is promising towards the optimization of WDPs for operation in near-zero-bias conditions.

Index Terms

Silicon photonics, Ge-on-Si pin waveguide photodetectors, electro-optic frequency response, multiphysics modeling.

I. Introduction

Silicon photonics [1], [2], allowing for the integration of optoelectronic components into CMOS-compatible platforms, has shown great promise in the development of next-generation telecommunication systems and fast, low-power data interconnects. Within this framework, the increasing transistor integration and power dissipation density has led, during the last decades, to a steady decrease of the CMOS bias voltages. This trend may also affect the operation of silicon photonics components: the present work is focused on the effects of lower bias in Ge-on-Si waveguide photodetectors (WPDs) [3]–[5], using the electro-optic (EO) frequency response [6, Sec. 4.9] as a figure of merit.

II. Structure, measurements and modeling approach

Two WPDs based on a vertical pin junction configuration have been considered, as shown in Fig. 1. The Ge absorber has been grown on top of a Si substrate; metallic contacts are placed on Si and Ge, allowing the reverse polarization of the device. Si is highly p-doped, while Ge is assumed intrinsic, with the exception of an highly doped n-type region at the metal/Ge interface. The Si optical waveguide is connected to the substrate with a long taper. The 3D multiphysics modeling approach is based on Synopsys RSoft FullWAVE [7], which provides the solution of the electromagnetic (EM) problem, and Synopsys TCAD Sentaurus [8], which solves the electrical transport problem. The model parameters have been reported in [9]–[11], while material properties follow [12]. The EM simulation propagates the light of a monochromatic source in the optical taper towards the Ge absorbing layer. The resulting optical generation rate distribution $G_{\text{opt}}(x, y, z)$ is used as a source term in the electrical simulation. Cisco Photonics carried out the experimental characterization. This involved measurements of the ratio of the output electrical modulation current and the input optical modulation power, using a Keysight Lightwave Component Analyzer (LCA) [13] on two groups of nominally identical samples (DUT), five for each of the two considered geometries (Device 1 and Device 2, see Fig. 1). The experimental results have been deembedded in order to remove the contribution of the measurement pads, while a Savitzky-Golay filter [14] has been applied to reduce high frequency noise contributions.

III. Results

A comparison between simulated and measured frequency response of Device 1 (DUT 5) at a wavelength $\lambda = 1310\,\text{nm}$ for three different bias values is reported in Fig. 1 (right). Fig. 2 shows the simulated EO cutoff frequency f_c as a function of the applied bias for both Device 1 and Device 2 and its experimental counterpart for all the corresponding DUTs. Our 3D simulations assume an input optical power $P_{\text{opt}} = 200\,\mu\text{W}$ ($-6.98\,\text{dBm}$) at the end of the taper. This assumption is compatible with the experimental P_{opt}, since the measured laser output power was -1.89 dBm (647 μW), with estimated waveguide losses of 5 dBm. The small-signal measurements were performed from 10 MHz to 50 GHz. An excellent agreement is observed for Device 1 at all the considered bias points, with a maximum absolute difference between simulated and experimental f_c (averaged over all the DUTs) smaller than 5 GHz. The larger difference observed for Device 2 could be explained by the sensitivity of f_c to the lateral extension of the implanted region W_{doping}, which in the DUTs is probably larger than the nominal value used in the simulations. The consistency between experiments and 3D multiphysics model will be explored on a wider set of nominal device geometries and, if confirmed, could be exploited in the optimization of vertical pin junction WPDs for low-bias operation.

ACKNOWLEDGEMENTS

This work was supported in part by Cisco Systems, Inc., under the Sponsored Research Agreement CONCERTI.

REFERENCES

[1] L. Pavesi, D. J. Lockwood, *Silicon Photonics* (Springer-Verlag, Berlin, 2004).
[2] D. J. Lockwood, L. Pavesi, *Silicon Photonics II. Components and Integration* (Springer-Verlag, Berlin, 2011).
[3] H. T. Chen, *et al.*, *J. Lightwave Technol.* **33**, 820 (2015).
[4] D. Benedikovic, *et al.*, *Photon. Res.* **7**, 437 (2019).
[5] M. de Cea, D. Van Orden, J. Fini, M. Wade, R. J. Ram, *APL Photon.* **6**, 041302 (2021).
[6] G. Ghione, *Semiconductor Devices for High-Speed Optoelectronics* (Cambridge University Press, Cambridge, U.K., 2009).
[7] Synopsys, Inc., Inc., Optical Solutions Group, Ossining, NY, *RSoft FullWAVE User Guide, v2019.09* (2019).
[8] Synopsys, Inc., Mountain View, CA, *Sentaurus Device User Guide. Version N-2017.09* (2017).
[9] A. Palmieri, *et al.*, *Opt. Quantum Electron.* **50**, 71 (2018).
[10] M. Vallone, *et al.*, *17th International Conference on Numerical Simulation of Optoelectronic Devices (NUSOD 2017)* (Copenhagen, Denmark, 2017), pp. 207–208.
[11] A. Palmieri, *et al.*, *20th International Conference on Numerical Simulation of Optoelectronic Devices (NUSOD 2020)* (online, 2020), pp. 27–28.
[12] V. Sorianello, *et al.*, *Opt. Mater. Express* **1**, 856 (2011).
[13] Keysight Technologies, Santa Rosa, CA, *Lightwave Component Analyzer application notes* (2017).
[14] A. Savitzky, M. J. E. Golay, *Anal. Chem.* **36**, 1627 (1964).

	W_{Ge}	H_{Ge}	L_{Ge}	W_{doping}	W_{metal}	W_{taper}
Device 1	4 μm	0.8 μm	15 μm	3 μm	1.5 μm	2.0 μm
Device 2	2 μm	0.8 μm	15 μm	1.5 μm	1.0 μm	1.5 μm

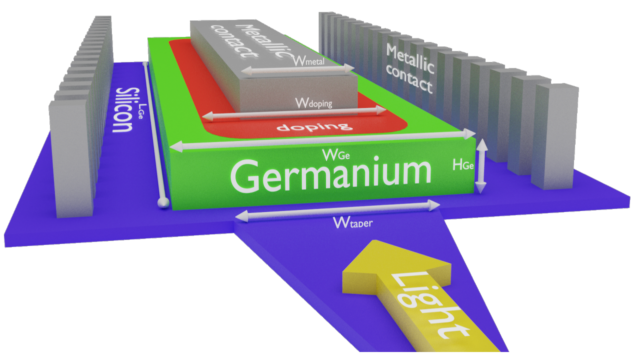

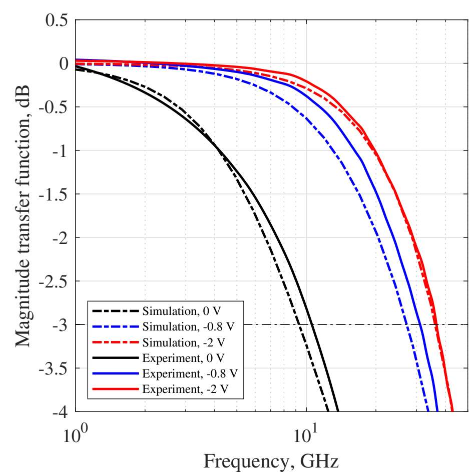

Fig. 1. Perspective view of the photodetector geometry (left); EO frequency response of Device 1 for different applied biases: simulations vs. measurements on a single device (DUT5) (right).

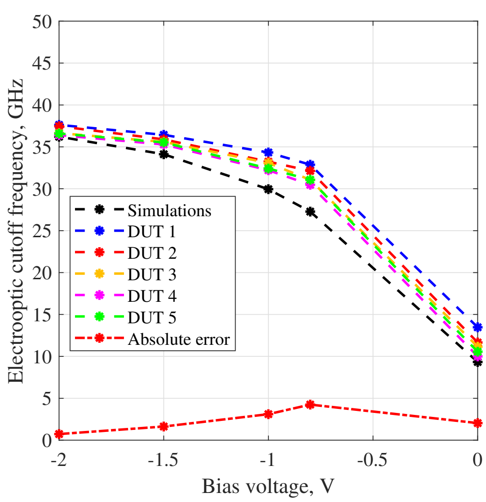

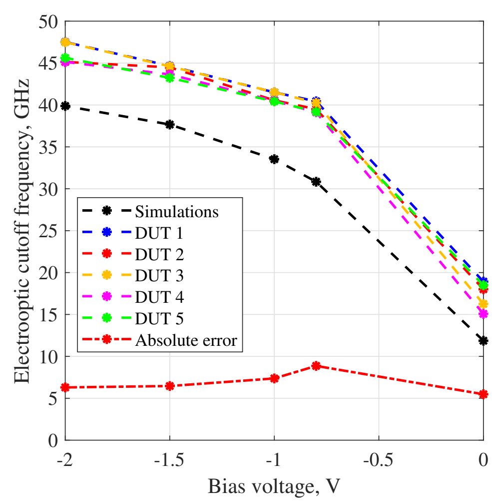

Fig. 2. Cutoff frequency f_c as a function of the applied bias: numerical simulations vs. measurements on all the nominally identical samples for Device 1 (left) and Device 2 (right). For both geometries, the difference between simulated f_c and corresponding experimental values averaged over all the DUTs is also reported.